COMPUTER SIMULATION OF ELECTRON SPIN RESONANCE SPECTRA OF $Ge_{25}S_{75}$ AND $Ge_{30}S_{70}$ BULK GLASSES

Zdenek CERNOSEK[a1], Marek LISKA[b], Peter PELIKAN[c1], Eva CERNOSKOVA[d], Marian VALKO[c2] and Miloslav FRUMAR[a2]

[a] *Department of General and Inorganic Chemistry, Faculty of Chemical Technology, University of Pardubice, 532 10 Pardubice, Czech Republic; e-mail: [1] cernosek@hlb.upce.cz, [2] frumar@hlb.upce.cz*

[b] *Institute of Inorganic Chemistry, Slovak Academy of Sciences, 911 01 Trencin, Slovak Republic; e-mail: liska@uanch1.savba.sk*

[c] *Department of Physical Chemistry, Faculty of Chemical Technology, Slovak Technical University, 812 37 Bratislava, Slovak Republic; e-mail: [1] pelikan@theochem.chtf.stuba.sk, [2] valko@theochem.chtf.stuba.sk*

[d] *Joint Laboratory of Solid State Chemistry of the Academy of Sciences of the Czech Republic and University of Pardubice, 530 09 Pardubice, Czech Republic; e-mail: cernosko@pol.upce.cz*

Received March 3, 1997
Accepted July 22, 1997

The electron spin resonance (ESR) spectra of bulk glasses of the chemical composition $Ge_{25}S_{75}$ and $Ge_{30}S_{70}$ were measured at liquid nitrogen temperature and subjected to computerized separation. The complex ESR spectra of both glasses were found to represent a superposition of three paramagnetic defect spectra, two with orthorhombic tensors $\boldsymbol{g}$ and one with the axial tensor $\boldsymbol{g}$. The former two paramagnetic centers can be related to a two-atomic defect of the sulfur–sulfur type, the latter to a germanium–sulfur defect. The experimental results are in a good agreement with the non-dangling bond model of paramagnetic defects in Ge–S glasses.

Key words: Electron spin resonance; ESR; EPR spectroscopy; Computer simulation; Paramagnetic defects; Ge–S glasses.

After Arai and Namikawa[1] discovered the intrinsic paramagnetic defects in the bulk glassy system Ge_xS_{100-x} ($20 \le x \le 42.55$) in 1973, considerable attention was paid to the analysis of the ESR spectra of this system. This special interest was stimulated by the fact that in contrast to a number of chalcogenide glasses such as Ge–Se, As–S, As–Se, the Ge–S glassy system contains dark intrinsic paramagnetic stable defects even at temperatures higher than room temperature. The term "dark intrinsic defects" means defects which are present in the melt in a thermal equilibrium and remain frozen-in on vitrification, in contrast to defects which are additionally induced in the glasses by light or γ radiation.

With respect to their shape, ESR spectra of Ge_xS_{100-x} glasses can be divided into two groups: multi-line spectra for glasses with an overstoichiometry of sulfur ($x < 33.33$), and single-line symmetric signals for the compound GeS_2 and glasses with $x > 33.33$.

This division led to the straightforward idea that the multi-line spectra are related to sulfur-atom defects whereas the single-line spectra are due to germanium defects, *e.g.* (refs[1,2]). The non-existence of dark-ESR spectra for other chalcogenide glasses and amorphous chalcogenides as mentioned above has been explained by a negative correlation energy following from the Kastner–Adler–Fritzsche (KAF) model[3]. A brief survey of some models of paramagnetic centers in the Ge–S glassy system has been presented in ref.[4].

The compositional dependence of the dark-ESR spectra of the Ge–S bulk glassy system and similarity between the photoinduced spectrum of amorphous sulfur and the spectra of sulfur-rich Ge–S glasses led to the development of the non-dangling bond model of intrinsic paramagnetic defects[4]. While the dangling bond assumes that the unpaired electron after bond-breaking is localized in the non-bonding atomic orbital of the one-atomic defect, the non-dangling bond model is based on the idea that the covalent (or slightly ionic) bond breaks in the first step and the dangling bonds created interact with the lone-pair electrons of sulfur, forming in the second step a two-atomic defect with the unpaired electron localized in the antibonding molecular orbital of this defect (for more detail see ref.[4]). One of the differences between the two models is that in Ge–S glasses with sulfur overstoichiometry the dangling bond model assumes sulfur-atom related defects solely because a dangling bond at the germanium atom is unlikely in sulfur-rich Ge–S glasses, whereas the non-dangling bond model predicts that paramagnetic defects associated with germanium defects should also exist in sulfur-rich Ge–S glasses. It is clear that a detailed analysis of the complex multi-line ESR spectra is the first step in elucidating the nature of the relatively very stable paramagnetic defects in Ge–S glasses.

The main aim of this work was to apply a numerical procedure to the analysis of complex "powder" ESR spectra and to verify the predicted[4] existence of the third type paramagnetic defect in sulfur-rich Ge–S glasses, thus providing experimental support to the non-dangling bond model of paramagnetic defect centers. Bulk glasses of the chemical composition of $Ge_{25}S_{75}$ and $Ge_{30}S_{70}$ were studied. Computer simulation of their dark-ESR spectra enables the trend of the concentration dependence of their components to be assessed.

EXPERIMENTAL

Methods

Five-gram samples of bulk $Ge_{25}S_{75}$ and $Ge_{30}S_{70}$ glasses were prepared by conventional direct synthesis from elements of semiconductor purity (5N). The elements (Ge: 2.15041 g, 29.62 mmol; S: 2.84959 g, 88.87 mmol for $Ge_{25}S_{75}$ and Ge: 2.46225 g, 33.92 mmol; S: 2.53775 g, 79.15 mmol for $Ge_{30}S_{70}$) were weighed into silica ampoules, evacuated and sealed. The reaction was conducted in a rocking electric furnace at 1 050 °C (24 h), and the homogeneous melt in the ampoules was tempered by dipping into ice-water bath. The glasses prepared were yellow in colour. The non-crystalline nature of the glasses was checked by optical microscopy and X-ray diffraction analysis. Chemical analysis

of the glasses was performed on the surface and on a fracture surface; an X-ray dispersion analyzer Kevex (Germany) was also used. The results showed that the samples were homogeneous and their chemical composition corresponded to the formula Ge_xS_{100-x} (x = 25 and 30) with and accuracy of x ±0.1.

The ESR spectra of powdered samples of the two glasses under nitrogen were measured in the X-band on ESR 221 spectrometer (ZWG Berlin, Germany); temperature 83 K; modulation of magnetic field 100 kHz, modulation amplitude 1 . 10^{-3} T; microwave power 10 mW. The power was sufficiently lower than the saturation energy. The complex ESR spectra obtained were separated numerically into the individual components using a computer program based on a mathematical model, which is briefly described below. A detailed description of the model along with a discussion of the mathematical procedure is given in ref.[5].

Numerical Analysis of ESR Spectra

Complex ESR spectra can be interpreted with the help of computer fit analysis. The dependence of the experimental spectrum $Y(B)$ on the external magnetic field induction B can be expressed as a linear combination of the Lorentz derivation bands corresponding to the individual paramagnetic centers in sample $y_i(B)$

$$Y(B) = x_0 + \sum_i^n x_i y_i(B) \ , \tag{1}$$

where x_0 is a constant background, x_i (i = 1, n) are coefficients of linear combination which represent the relative quantities of the individual types of paramagnetic species, n is the number of different paramagnetic species in sample, and

$$y_i(B) = N_i \int_0^{\pi} \int_0^{\pi/2} P_i(\vartheta,\varphi) \frac{B - B_i^0(\vartheta,\varphi)}{\Delta B_i(\vartheta,\varphi)} \left\{1 + \frac{4[B - B_i^0(\vartheta,\varphi)]^2}{3\Delta B_i^2(\vartheta,\varphi)}\right\}^{-2} \sin\vartheta \cos\varphi \, d\vartheta \, d\varphi \ , \tag{2}$$

where N_i is the normalization constant satisfying the condition[6]

$$\int_0^{\infty} \int_0^{B} y_i(B') \, dB' \, dB = 1 \ . \tag{3}$$

The transition probability $P_i(\vartheta,\varphi)$ is given by the following equation[7]:

$$P_i(\vartheta,\varphi) = g_{x,i}^2 [g_{y,i}^2 \sin^2\vartheta + g_{z,i}^2 (\cos^2\varphi + \cos^2\vartheta \sin^2\varphi)] + g_{y,i}^2 g_{z,i}^2 (\sin^2\varphi + \cos^2\vartheta) \ . \tag{4}$$

The spectral line half-width $\Delta B_i(\vartheta,\varphi)$ is a complex function of the orientation of the paramagnetic particles (due to the relaxation time dependence on the anisotropy of the solid sample structure)[8]

$$\Delta B_i(\vartheta,\varphi) = \{[\Delta B_{x,i}^2 \cos^2\varphi + \Delta B_{y,i}^2 \sin^2\varphi] \sin^2\vartheta + \Delta B_{z,i}^2 \cos^2\vartheta\}^{1/2} \ . \tag{5}$$

For the resonance frequency we have[9]

$$B_i^0(\vartheta,\varphi) = \frac{h\nu}{g_{ef,i}(\vartheta,\varphi)\beta} \ , \tag{6}$$

where ν is the klystron frequency, h is the Planck constant, β is the Bohr magneton, and $g_{ef,i}$ is given by Eq. (*7*) (ref.[6]):

$$g_{ef,i}(\vartheta,\varphi) = \{[g_{x,i}^2 \cos^2 \varphi + g_{y,i}^2 \sin^2 \varphi] \sin^2 \vartheta + g_{z,i}^2 \cos^2 \vartheta\}^{1/2} \ . \tag{7}$$

For axially symmetric ESR spectra we have

$$g_{x,i} = g_{y,i} = g_{\perp,i} \tag{8}$$

$$g_{z,i} = g_{\parallel,i} \tag{9}$$

$$\Delta B_{x,i} = \Delta B_{y,i} = \Delta B_{\perp,i} \tag{10}$$

$$\Delta B_{z,i} = \Delta B_{\parallel,i} \tag{11}$$

whereby all equations are simplified.

The best estimates of the n_p unknown parameters ($g_{\alpha,i}$, $\Delta B_{\alpha,i}$, x_i) can be obtained by minimization of the sum of squared deviations

$$F(\boldsymbol{p}) = \sum_{l}^{n_N} [Y^{\exp}(B_l) - Y^{\mathrm{calc}}(B_l)]^2 = \text{minimum} \, , \tag{12}$$

where $\boldsymbol{p}$ is the vector of the n_p unknown parameters, $Y^{\exp}(B_l)$ are experimentally measured spectral points and $Y^{\mathrm{calc}}(B_l)$ are spectral points calculated by Eq. (*1*).

If the experimental spectrum is normalized, *i.e.*

$$\int_0^\infty \int_0^B [Y^{\exp}(B') - x_0] \, \mathrm{d}B' \, \mathrm{d}B = 1 \ , \tag{13}$$

the following condition is fulfilled

$$\sum_{i=1}^{n} x_i = 1 \ . \tag{14}$$

The minimization task can be divided into two interconnected parts:

1. a non-linear minimization problem with regard to the spin Hamiltonian parameters, which are determined by the physical character of the problem solved;

2. a linear minimization problem with regard to the vector $\boldsymbol{x} = \{x_i\}$ for $i = 1, n$

$$\boldsymbol{x} = \{x_i\} \quad \text{for } i = 0, n \tag{15}$$

including the binding condition[10] and, simultaneously

$$x_i > 0 \quad \text{for } i = 1, n \ . \tag{16}$$

The linear minimization with respect to the vector is performed for each calculation of the F criterion, Eq. (*12*).

RESULTS AND DISCUSSION

The experimental ESR spectra and results of their numerical analysis are shown in Figs 1 and 2. The principal values of the tensor $\boldsymbol{g}$, half-height width ΔB_i and relative content of the individual components in the ESR spectrum corresponding to the concentrations of the paramagnetic defects are given in Table I.

As given above, two basic models of defect centres have been suggested[3,5]. One is based on the idea that the experimental ESR spectrum is a superposition of spectra of two kinds of sulfur-located defects[2]. The defects of the first kind can be schematically

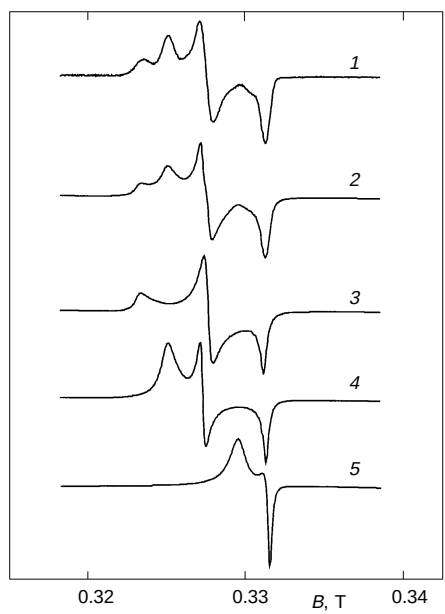

FIG. 1
ESR spectrum of $Ge_{25}S_{75}$ bulk glass (measured at microwave frequency = 9.289 GHz) and its computer simulation; *1* experimental spectrum, *2* computer-simulated spectrum, *3* DCIII spectrum, *4* DCII spectrum, *5* DCI spectrum

represented as Ge–S• (the dot denotes an unpaired electron in the non-bonding orbital located at the sulfur atom, so-called dangling bond), the defects of the second kind are similarly represented as Ge–S–S• (for an in-depth explanation see ref.[4]). A defect of the dangling-bond type located at the germanium atom is very improbable in the case of sulfur overstoichiometry, and therefore is omitted from this model.

The next model supposing localization of the unpaired electron in the anti-bonding molecular orbital is based on three experimental facts:

1. Paramagnetic defects in Ge–S glasses are relatively stable even at temperatures close to the glass transition temperature.

2. The mean value of the principal components of tensor $\boldsymbol{g}$ is substantially higher than the free electron value ($\boldsymbol{g}_e = 2.00232$), see Table I.

3. The photoinduced ESR spectrum of the non-crystalline sulfur represents a superposition of two spectra. The symmetry and the principal values of tensor $\boldsymbol{g}$ of the spectra are almost identical with those for the major components of the multi-line ESR spectra of sulfur-rich glasses in the Ge–S system, as shown in ref.[4].

Based on the first two experimental facts, it can be assumed that the presence of a dangling bond (*i.e.* unsaturated bond) is not very probable. The positive deviation of the mean value of the principal components of tensor $\boldsymbol{g}$ points to a localization of the electron in a more than half-occupied molecular orbital (anti-bonding molecular orbital) rather than in the non-bonding atomic orbital. The third experimental fact virtually rules out the model of the Ge–$(S)_n$–S• type (n = 0, 1), as it supposes a different length of the sulfur chains terminated by a branching germanium atom, which is not present in

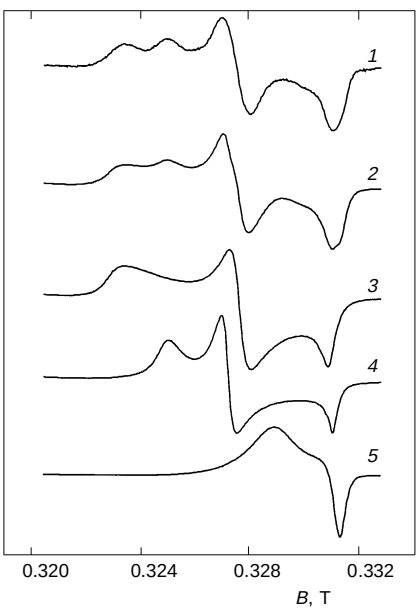

FIG. 2
ESR spectrum of $Ge_{30}S_{70}$ bulk glass (measured at microwave frequency = 9.289 GHz) and its computer simulation; *1* experimental spectrum, *2* computer-simulated spectrum, *3* DCIII spectrum, *4* DCII spectrum, *5* DCI spectrum

the non-crystalline sulfur. To account for the experimental results we have suggested[4] the non-dangling bond model assuming a coexistence of three two-atom defects. In the defects, two sulfur atoms or a sulfur and a germanium atom are connected by a bond whose formal order is 1/2 (the unpaired electron is located in the anti-bonding molecular orbital). The defect centres (DC) have been represented[4] using the conventional Kastner–Adler–Fritzsche-model notation (subscript means coordination, superscript charge, and dots, bond of order 1/2) as $(Ge_4\ldots S_3)^0$, $(S_2\ldots trans\text{-}S_3)^0$ and $(S_2\ldots cis\text{-}S_3)^0$, and for clarity denoted DCI, DCII, and DCIII, respectively. The DCII defect originates

TABLE I
Results of computer analysis of ESR spectra of $Ge_{25}S_{75}$ and $Ge_{30}S_{70}$ glasses (DC two-atomic paramagnetic defect centrum, g_i principal values of tensor $\boldsymbol{g}$, ΔB_i band half-width)

Defect	Parameter	Chemical composition	
		$Ge_{25}S_{75}$	$Ge_{30}S_{70}$
DCIII[a]	g_1	2.053	2.053
	g_2	2.026	2.025
	g_3	2.005	2.006
	ΔB_1, T	$4.1 \cdot 10^{-4}$	$6.2 \cdot 10^{-4}$
	ΔB_2, T	$3.4 \cdot 10^{-4}$	$3.9 \cdot 10^{-4}$
	ΔB_3, T	$3.2 \cdot 10^{-4}$	$3.8 \cdot 10^{-4}$
DCII[b]	g_1	2.043	2.043
	g_2	2.028	2.028
	g_3	2.004	2.005
	ΔB_1, T	$3.5 \cdot 10^{-4}$	$2.8 \cdot 10^{-4}$
	ΔB_2, T	$1.5 \cdot 10^{-4}$	$2.1 \cdot 10^{-4}$
	ΔB_3, T	$2.6 \cdot 10^{-4}$	$2.7 \cdot 10^{-4}$
DCI[c]	$g\|\|$	2.015	2.017
	$g_\perp$	2.002	2.003
	$\Delta B\|\|$	$1.7 \cdot 10^{-4}$	$2.1 \cdot 10^{-4}$
	$\Delta B_\perp$	$5.0 \cdot 10^{-4}$	$6.9 \cdot 10^{-4}$
		Relative concentration	
DCIII[a]		0.64	0.76
DCII[b]		0.33	0.17
DCI[c]		0.03	0.07

[a] $(S_2\ldots trans\text{-}S_3)^0$; [b] $(S_2\ldots cis\text{-}S_3)^0$; [c] $(Ge_4\ldots S_3)^0$. The subscript denotes the coordination of the atom, the superscript indicates the charge of the defect centre

from interaction of a sulfur atom dangling bond with lone-pair electrons of sulfur chains S_n (*trans*), and differs from DCIII which arises from interaction of the dangling bond with the electrons of sulfur cycles S_8 or their remains (*cis*). The DCI defect is supposed to result from interaction of the germanium atom dangling bond with lone-pair electrons of the sulfur atom. As the precursor of the DCI defect is located at the germanium atom, the concentration of this defect should decrease with increasing sulfur overstoichiometry, with a parallel increase in the concentrations of the DCII and DCIII defects.

The experimental ESR spectra of the two sulfur-rich glasses were considered as a superposition of spectra of two paramagnetic defects with orthorhombic tensors $\boldsymbol{g}$. The computer simulation of the spectra presented here shows that they are actually composed of three components, as shown in Figs 1 and 2 and Table I. The relative concentration of the newly found minor component corresponding to the defect having the axially symmetric tensor $\boldsymbol{g}$ decreases with increasing abundance of sulfur. This is consistent with the assumption described above for DCI. Simultaneously, the relative total concentration of DCII and DCIII defects increases as expected. Table I demonstrates that the DCII to DCIII defect ratio changes. The reduced concentration of DCIII and increased concentration of DCII at a higher sulfur overstoichiometry can be interpreted in terms of the change in the ratio of S_n chains to S_8 cycles or their fragments. Based on IR and Raman spectral study[11], it has been suggested for Ge–S glasses with a low sulfur overstoichiometry (not exceeding a few percent) that only S_n chains are present and the S_8 cycle content increases with increasing sulfur overstoichiometry more rapidly than the chain content. Therefore, we believe that the interpretation of the change in the concentrations of the DCII and DCIII defects suggested by us is realistic. A major consequence of this is that the DCII defect is probably $(S_2\ldots\textit{cis}\text{-}S_3)^0$ type and the DCIII defect $(S_2\ldots\textit{trans}\text{-}S_3)^0$ type, contrary to the previous assumptions[4] outlined above, which were based on qualitative estimates.

CONCLUSIONS

The computer analysis of ESR spectra of two glasses in the Ge–S system with sulfur overstoichiometry confirmed that three paramagnetic defects exist in the glasses, whereby the non-dangling bond model of paramagnetic defects in Ge–S glasses[4] is experimentally supported. It has been shown that the assignment of the DCII and DCIII defects with respect to the geometrical isomerism of the sulfur atom chain fragments should be changed. The computer simulation of multi-line ESR spectra of glasses in the Ge–S system that have not been analyzed in detail until now confirmed applicability of the numerical approach to the optimization of the parameters of the spin Hamiltonian for a system with more randomly orientated paramagnetic species in the solid state, leading to an acceptable solution of the problem.

LIST OF SYMBOLS

B, B'	external magnetic field induction
ΔB_i	spectral line half-width
DC	defect centrum
$F(\boldsymbol{p})$	sum of squared deviations, *F*-criterion, Eq. (*12*)
$\boldsymbol{g}$	tensor
g_e	free electron *g*-value
$g_{k,i}$	principal value of tensor $\boldsymbol{g}$
h	Planck constant
KAF	Kastner–Adler–Fritzsche model (valence-alternation pair model)
N_i	normalization constant, Eq. (*2*)
n	number of different paramagnetic species
n_p	number of unknown parameters, Eq. (*12*)
P_i	transition probability, Eq. (*4*)
$\boldsymbol{p}$	vector of n_p unknown parameters
x_i	coefficient of linear combination
x_0	constant background
$\boldsymbol{x}$	vector of coefficients of linear combination
$Y(B)$	experimental ESR spectrum
$Y^{calc}(B_i)$	theoretically calculated spectral point
$Y^{exp}(B_i)$	experimentally measured spectral point
$y_i(B)$	derivation band of individual paramagnetic centre
β	Bohr magneton
ϑ, φ	Euler angles
ν	klystron frequency

This work was supported by the grants No. 203/96/0184 and No. 203/96/0876 of the Grant Agency of the Czech Republic and No. 1171/96 of the Slovak Grant Agency for Science.

REFERENCES

1. Arai K., Namikawa H.: Solid State Commun. *13*, 1167 (1973).
2. Watanabe Y., Kawazoe H., Yamane M.: Phys. Rev. B: Condens. Matter *38*, 5668 (1988).
3. Kastner M., Adler D., Fritzsche H.: Phys. Rev. Lett. *37*, 1504 (1976).
4. Cernosek Z., Cernoskova E., Frumar M., Swiatek K.: Phys. Status Solidi B *192*, 181 (1995).
5. Pelikan P., Liska M., Valko M., Mazur M.: J. Magn. Reson., Ser. A *122*, 9 (1996).
6. Gordy W. in: *Theory and Applications of Electron Spin Resonance* (A. Weissberger, Ed.), p. 355. McGraw–Hill, New York 1972.
7. Taylor P. C., Baugher J. F.: Chem. Rev. *75*, 203 (1975).
8. Pilbrow J. R., Winfield M. E.: Mol. Phys. *25*, 1073 (1973).
9. Swalen J. D., Gladney H. M.: IBM J. Res. Dev. *77*, 852 (1950).
10. Pelikan P., Ceppan M., Liska M. in: *Applications of Numerical Methods in Molecular Spectroscopy* (S. R. Brown, Ed.), p. 341. CRC Press, London 1994.
11. Lucovsky G., Galeener F. L., Keezer R. C., Geils R. H., Six H. A.: Phys. Rev. B: Solid State *10*, 5134 (1974).